Available online at www.sciencedirect.com
SCIENCE DIRECT®
Polyhedron 24 (2005) 949–957
POLYHEDRON
www.elsevier.com/locate/poly

Synthesis and antimicrobial activity of copper(II) and silver(I) complexes of hydroxynitrocoumarins: X-ray crystal structures of $[Cu(hnc)_2(H_2O)_2] \cdot 2H_2O$ and [Ag(hnc)] (hncH = 4-hydroxy-3-nitro-2*H*-chromen-2-one)

Bernadette S. Creaven [a,*], Denise A. Egan [a], Kevin Kavanagh [b], Malachy McCann [c], Mary Mahon [d], Andy Noble [a], Bhumika Thati [a], Maureen Walsh [a]

[a] *Department of Applied Science, Institute of Technology, Tallaght, Dublin 24, Ireland*
[b] *Department of Biology, National University of Ireland, Maynooth, Co. Kildare, Ireland*
[c] *Department of Chemistry, National University of Ireland, Maynooth, Co. Kildare, Ireland*
[d] *X-ray Crystallographic Suite, Department of Chemistry, University of Bath Claverton Down, Bath BA2 7AY, UK*

Received 26 January 2005; accepted 7 March 2005
Available online 29 April 2005

Abstract

$[Cu(hnc)_2(H_2O)_2] \cdot 2H_2O$ (**1**) [hncH = 4-hydroxy-3-nitro-*2H*-chromen-2-one] and [Ag(hnc)] (**2**) were prepared by deprotonating the hydroxy group of hncH with NaOH and then adding copper(II) chloride dihydrate and silver(I) nitrate, respectively. [Ag(hmnc)] (**3**) was synthesised in a similar manner [hmncH = 7-hydroxy-8-nitro-3-methyl-*2H*-chromen-2-one]. The mixed-ligand Ag(I) complex $[Ag(phen)_2hnc]$ (**4**) was prepared by treating silver(I) nitrate with 1,10-phenanthroline (phen) (1:1) and subsequent reaction with a solution containing hncH and NaOH. Molecular structures of **1** and **2** were determined by X-ray crystallography. The asymmetric unit in **1** contains two molecules of water in addition to one molecule of the copper complex. In **2** the asymmetric unit comprises one hnc^- ligand moiety bonded in a bidentate fashion to the silver(I) ion with additional interactions from three other coumarin ligands. The geometry is best described as pentagonal bipyramidal. While none of the coumarin-based ligands or the free copper salt showed any significant anti-microbial activity, $AgNO_3$ and its' phen and coumarin complexes exhibited good anti-microbial activity, particularly against the clinically important methicillin-resistant *Staphylococcus aureus* (MRSA) bacterium and also demonstrated good activity, comparable to that of the commercial fungicides clortrimazole and ketoconazole, against a clinical isolate of the fungal pathogen *Candida albicans*.

Keywords: Coumarin; Copper(II); Silver(I); Anti-microbial; X-ray structure; *Candida albicans*

1. Introduction

Interest in coumarin chemistry has flourished for many years, largely as a result of the wide spectrum of uses for coumarin derivatives. Such derivatives have been proven to function as anti-coagulants [1], antibacterial agents [2], antifungal agents [3], biological inhibitors [4], chemotherapeutics [5] and as bio-analytical reagents [6]. Recently, an area of coumarin chemistry that is increasing in importance concerns biologically active metal complexes of coumarin-based ligands. In general, coordination of metal ions to therapeutic agents improves their efficacy and accelerates

* Corresponding author. Tel.: +14042889; fax: +14042700.
E-mail address: bernie.creaven@it-tallaght.ie (B.S. Creaven).

0277-5387/$ - see front matter © 2005 Elsevier Ltd. All rights reserved.
doi:10.1016/j.poly.2005.03.006

bioactivity. In this context, a broad array of medicinal applications of metal complexes has been investigated and several recent reviews summarize advances in this field [7–12]. Previous studies have been carried out on the chemotherapeutic and anti-microbial activity of a limited number of metal-coumarin complexes. Kumar et al. [13,14] synthesised a number of hydroxy-substituted coumarin transition metal complexes, which included a series of complexes of hydroxynitrocoumarins, hydroxyaminocoumarins, 4-hydroxy-3-phenylazocoumarin and 8-acetyl-4-methylumbelliferone. The complexes were tested for their antifungal ability using *Rhizoctonia solani* (causative organism for sheath blight in rice plants) and also against the bacterial strain *Escherichia coli*. Their results demonstrated that metal complexes displayed greater inhibition of microbial growth than free ligands and, furthermore, activity was comparable to that of the commercial bactericide, Agrimycin-100. Kostova et al. [15–20] have carried out a series of studies on the cytotoxicity of lanthanide and zirconium complexes of hydroxylated coumarins and reported IC_{50} values of 50–300 μM for the neodymium complexes of bis-coumarins when screened using HL-60, Hl-60/Dox and SKW-3 cell lines. A recent study by Nath et al. [21] has shown that triorganotin(IV) derivatives of 7-hydroxycoumarin, and their adducts with 1,10-phenanthroline (phen), have potent anti-inflammatory activity.

We have previously studied the chemotherapeutic potential of a series of metal-free hydroxynitrocoumarins [22–27]. These compounds were tested against both normal human and neoplastic skin cell lines and were found to be selectively cytotoxic to human skin malignant melanocytes and renal cell carcinoma. An earlier study had found that 7-hydroxy-8-nitrocoumarin was cytotoxic to a panel of cell lines including K562 (human erythroleukemic), HL-60 (human promyelocytic) and CHrC5 (Chinese hamster ovary) [28]. It was thought that the biological activity exhibited by the compounds could be increased by their coordination to a metal centre and a study to investigate this proposal is currently underway. However, a tandem study on the antimicrobial activity of a series of these metal complexes was carried out given the results obtained by Kumar et al. [13,14] on related coumarin complexes.

The present paper details the synthesis of a Cu(II) and a number of Ag(I) hydroxynitrocoumarin complexes and their subsequent in vitro screening against a range of Gram positive and Gram negative bacterial strains and also against a clinical isolate of *Candida albicans*. In addition, a silver(I) complex containing hydroxynitrocoumarin and phen ligands also isolated and its anti-microbial activity was investigated.

2. Experimental

2.1. Chemistry

Chemicals and solvents were purchased from Sigma–Aldrich Co. (Dorset, UK), with the exception of 4-methyl-7-hydroxy-8-nitro-chomen-*2*-one (hmncH) which was obtained from Lancaster (Lancashire, UK) and used without further purification. Infrared spectra of solids (in a KBr matrix) were recorded in the region 4000–400 cm^{-1} on a Nicolet Impact 410 Fourier-Transform Infrared spectrophotometer. A JEOL JNM-LA300 FT-NMR spectrometer was used to record ^1H NMR spectra (−5 to 15 ppm from TMS) and ^{13}C NMR spectra (−33 to 233 ppm from TMS) as solutions in d^6-DMSO. Microanalytical data were provided by the Microanalytical Laboratory, National University of Ireland, Belfield, Dublin 4. Solid state magnetic susceptibility measurements were carried out at room temperature in the Dublin Institute of Technology, Cathal Brugha Street, Dublin 1, using a Johnson Matthey Magnetic Susceptibility Balance with $[HgCo(SCN)_4]$ being used as a reference standard.

2.1.1. $[Cu(hnc)_2(H_2O)_2]\cdot 2H_2O$ (*1*)

A solution of $CuCl_2\cdot 2H_2O$ (0.082 g, 0.48 mmol) in water (10 cm^3) was added to a solution of NaOH (0.04 g, 0.97 mmol) and 4-hydroxy-3-nitro-*2H*-chromen-2-one (hncH) (0.20 g, 0.97 mmol) in water (10 cm^3) and the mixture left to stir for 2 h. After standing for 2 days, a green product precipitated which was filtered off, washed with cold water and methanol and then dried in a vacuum oven at 40 °C. The solid was recrystallised from water. Yield: 0.20 g (81%). The complex was soluble in DMSO, and sparingly soluble in ethanol, methanol and water. *Anal.* Calc. C, 42.24; H, 2.32; N, 5.47; Cu, 12.77. Found: C, 43.04; H, 2.08; N, 5.27; Cu, 12.46%. IR (KBr): 3471, 3447, 2950, 1686, 1671, 1613, 1552, 1467, 1376, 1343, 1281, 1261, 1212 cm^{-1}. μ_{eff} = 2.01 BM.

2.1.2. $[Ag(hnc)]$ (*2*)

A solution of $AgNO_3$ (0.164 g, 0.96 mmol) in water (10 cm^3) was added to a solution of NaOH (0.04 g, 0.97 mmol) and hncH (0.20 g, 0.97 mmol) in water (10 cm^3) and the mixture left to stir for 2 h. Upon standing a yellow precipitate formed, which was filtered off, washed with methanol and cold water and then dried under vacuum at 40 °C. The solid was recrystallised from water. Yield: 0.14 g (46%). The complex was soluble in DMSO, and sparingly soluble in methanol, ethanol and water. *Anal.* Calc. C, 34.42; H, 1.28; N, 4.46%. Found: C, 34.33; H, 1.16; N, 4.28%. ^1H NMR: Ar–H5 (7.88 ppm, 1H, ddd, J = 7.88, 1.83, 0.36 Hz), Ar–H6 (7.22 ppm, 1H, brd, J = 7.53 Hz), Ar–H7 (7.51 ppm,

1H, dt, $J = 8.61$, 7.5, 1.83 Hz) Ar–H8 (7.17 ppm, 1H, ddd, $J = 8.82$, 1.11, 0.36 Hz); ^{13}C NMR: C2, 167.6; C3, 120.47; C4, 152.44; C4a, 122.29; C5, 125.59; C6, 122.89; C7, 132.08; C8, 116.02; C8a, 157.58 ppm. IR (KBr): 1687, 1610, 1584, 1462, 1434, 1347, 1308, 1286 cm^{-1}.

2.1.3. [Ag(hmnc)] (3)

A solution of $AgNO_3$ (0.169 g, 0.995 mmol) in water (10 cm^3) was added over a period of 10 min to a solution of NaOH (0.04 g, 0.97 mmol) and hmncH (0.20 g, 0.90 mmol) in water (10 cm^3) at room temperature. A brown/red solid immediately precipitated and the resulting suspension was left to stir for 1 h. The solid was filtered off, washed with cold water and dried under vacuum at 40°C. Yield: 0.180 g (61%). The complex was soluble in DMSO and insoluble in all other common solvents. *Anal.* Calc. C, 36.16; H, 1.84; N, 4.27. Found: C, 37.08; H, 1.80; N, 4.15%. ^1H NMR: CH_3 (2.3 ppm, 3H, d, $J = 0.7$ Hz), Vinyl–H, (5.7 ppm, 1H, d, $J = 0.7$ Hz), Ar–H5 (6.3-7.3 ppm, 1H, d, $J = 9.3$ Hz), Ar–H6 (6.33 ppm, 1H, d, $J = 9.3$ Hz) ^{13}C NMR: C2, 166.44; C3, 103.0; C4, 159.81; C4a, 102.38; C5, 125.9; C6, 120.3; C7, 154.48; C8, 130; C8a, 148.21; CH_3, 18 ppm. IR (KBr): 3412, 1719, 1617, 1588, 1541, 1506, 1420, 1369, 1329, 1276 cm^{-1}.

2.1.4. [Ag(phen)$_2$hnc] (4)

A solution of $AgNO_3$ (0.123 g, 0.72 mmol) in water (10 cm^3) was added to a solution of phen (0.131 g, 0.72 mmol) in ethanol (10 cm^3) giving an immediate yellow precipitate. This suspension was then added to a solution comprising hncH (0.15 g, 0.72 mmol) and NaOH (0.029 g, 0.72 mmol) in water (10 cm^3) over a 10 min period at room temperature. The mixture was then refluxed for 1 h and the resulting yellow solid was filtered off, washed with cold water and dried under vacuum at 40 °C. Yield: 0.180 g (74%). The complex was soluble in DMSO, methanol and ethanol and sparingly soluble in water. *Anal.* Calc. C, 58.7; H, 2.98; N, 10.38. Found: C, 57.7; H, 2.94; N, 9.96%. ^1H NMR: Phen–H H2, (9.17 ppm, 4H, dd, $J = 4.6$, 1.6 Hz), H3, (8.01 ppm, 4H, dd, $J = 4.6$, 8.2 Hz), H4, (8.78 ppm, 4H, dd, $J = 1.6$, 8.3 Hz) H5 (8.22 ppm, 4H, s) hnc protons Ar–H5 (7.86 ppm, 1H, ddd, $J = 7.7$, 1.8, 0.4 Hz) Ar–H6 (7.20 ppm, 1H, dt, $J = 7.7$, 1.11 Hz) Ar–H7 (7.49 ppm, 1H, dt, $J = 8.61$, 1.7 Hz), Ar–H8 (7.47 ppm, 1H, dd, $J = 8.6$, 1.1 Hz) IR (KBr): 3442, 1685, 1619, 1570, 1509, 1462, 1421, 1297, 1208 cm^{-1}.

2.2. Antifungal susceptibility testing

A clinical isolate of *C. albicans* ATCC 10231 was obtained from American Type Culture Collection (Maryland, USA). Antifungal susceptibility testing was performed using broth microdilution assays according to the National Committee for Clinical Laboratory standards (Document M27-A2) protocol with slight modifications. M27-A2 method was altered by substituting Antibiotic Medium 3 (Oxoid Ltd.) for RPMI 1640 medium. Using this method minimum inhibitory concentrations (MICs) were determined by UV spectrophotometer at 405 nm by comparing the turbidity of growth in each well. MIC_{80} is defined as the lowest concentration of drug that inhibits growth by 80%.

2.3. Anti-microbial testing

All bacterial isolates were obtained from clinical samples: *Staphylococcus aureus* (urinary track infection), methicillin-resistant *S. aureus* (wound infection), *Staphylococcus simulans* (facial skin), *Micrococcus luteus* (facial skin) *E. coli* (gastro-intestinal tract), *Bacillus oleronius* (facial skin), *Pantoea agglumerans* (facial skin). The Gram-positive strains used were *S. aureus* (SA), *methycillin-resistant S. aureus* (MRSA), *S. simulans* (S.Sim.) and *M. luteus* (Ml) and the Gram negative strains were *E. coli* (E.Coli), *B. oleronius* (BO) and *P. agglumerans* (PA).

The coumarin complexes were tested against four Gram positive and three Gram negative strains to determine their antibacterial activity. Bacterial strains were grown overnight in nutrient broth medium at 30 °C and 200 rpm in an orbital incubator. The absorbance of these cultures was measured at 660 nm and cultures were diluted to an optical density of 0.1. The cell suspension (100 μl) was added to the wells of a 96 well plate containing novel coumarin derivative dissolved in nutrient broth medium in serial dilutions from 100 to 0.25 μg/ml. Plates were incubated at 30 °C for 24 h and the optical density was measured spectrophotometrically (Dynex Technology) at 660 nm.

3. Results and discussion

3.1. Complex synthesis and spectral characterisation

$[Cu(hnc)_2(H_2O)_2] \cdot 2H_2O$ (**1**) and [Ag(hnc)] (**2**) were prepared in aqueous solution by deprotonating the hydroxy group of hncH with NaOH and then adding copper(II) chloride dihydrate and silver(I) nitrate, respectively. [Ag(hmnc)] (**3**) was synthesised in a similar manner. The mixed-ligand Ag(I) complex [Ag(phen)$_2$hnc] (**4**) was prepared by treating silver(I) nitrate with phen (1:1) and subsequent reaction with a solution containing hncH and NaOH.

The infrared spectra of the complexes and free ligands were recorded in KBr matrix. The most significant changes in absorption frequencies between the

free and coordinated ligands are the $\nu_{asym}(NO_2)$ stretch of the nitro group, the ν(C=O) and ν(C–O) stretches of the lactone (in hncH), and the phenoxy alcohol ν(O–H) stretch (in hmncH). The values for the ν_{asym} nitro for all of the complexes (ca. 1580 cm^{-1}), when compared with that of the free ligand (ca. 1535 cm^{-1}), have all increased, but the effect on ν_{sym} nitro is more difficult to determine as there are many overlapping bands in this region. The ν_{C-O} stretch of the alcohol on both the lactone (in hncH) and the phenoxy (in hmncH) rings also decreased by 80–100 cm^{-1} upon formation of the complexes. Both of these shifts would be consistent with bonding to the metal being through the nitro and hydroxyl/phenoxy oxygen groups, to form a 6-membered chelate ring. There was also a significant shift in the $\nu_{C=O}$ bond, which lowers by ca. 60 cm^{-1} upon complexation for the hncH complexes but hardly at all for the hmncH complex. This is not too surprising,as in the hncH complexes the carbonyl is located on the same lactone ring as the ligand binding site. Such a large shift in $\nu_{C=O}$ in similar complexes has been taken as evidence that complexation occurs through the carbonyl oxygen atom [15–20]. It has recently been shown that, in the case of 7-hydroxy-4-methylcoumarin complexes of Na^+, Cu^+ and H^+, where bonding is through the phenolate anion, coordination to the cation induced polarisation on the lactone ring and resulted in significant shifts in the carbonyl stretching frequency [31]. In the mixed-ligand species **4** distinctive bands for the phen ligand were evident at 1421, 853 and 738 cm^{-1}.

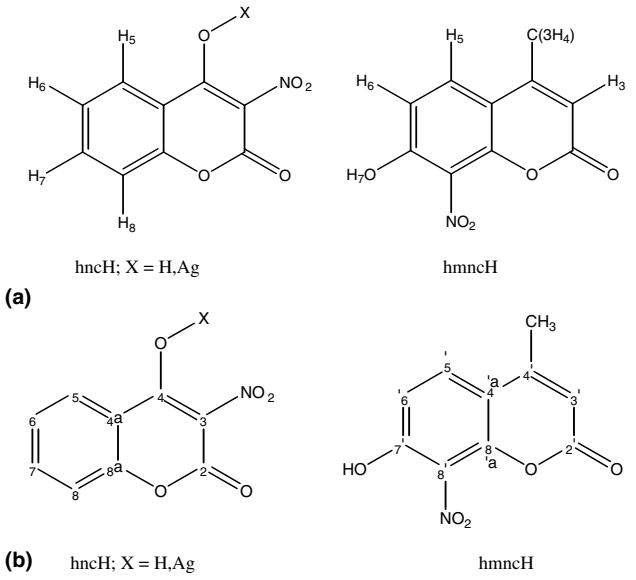

Fig. 1. Structures of the hncH and hmncH ligands used in this study showing atom numbering used in (a) ^{1}H NMR spectral assignments and (b) ^{13}C NMR spectral assignments.

The ^{1}H NMR solution spectra of the Ag(I) complexes show resonance shifts for all of the complexes relative to the uncoordinated ligand (see Fig. 1 for atom numbering). For the hncH complexes, coordination through the nitro and phenoxy oxygen atoms of the lactone ring results in upfield shifts of between 0.03 and 0.06 ppm for the protons on the fused aromatic ring, particularly so for the mixed hncH–phen complex **4**. Also of note is the disappearance of the exchangeable hydrogen peak for the now deprotonated and coordinated hydroxy oxygen atom of the complexed ligands. The ^{13}C NMR spectra show that the carbon atoms on the lactone ring which is attached to the nitro groups experience the most significant downfield shift (ca. 40 ppm) upon coordination of the Ag(I) cation.

The ^{1}H NMR spectrum of the Ag(I) hmncH complex **3** shows significant downfield shifts (ca. 0.15–0.7 ppm) for all protons, particularly those on the aromatic ring, when compared to the metal-free ligand. Similar shifts were noted in the ^{13}C NMR spectrum, with the largest being for the carbon atoms attached to the hydroxy and nitro groups (−15 and +40 ppm, respectively). There was no significant shift observed for the carbonyl carbon atom upon coordination to the metal. The ^{1}H NMR spectrum of the hncH–phen complex **4** has additional signals at 9.18, 8.80, 8.05 and 8.00 ppm corresponding to the presence of the two phen ligands and the integrals confirm the 2:1 phen:coumarin ratio.

3.2. X-ray crystal structure of $[Cu(hnc)_2(H_2O)_2] \cdot 2H_2O$ (1)

The X-ray crystal structure of **1** is shown in Fig. 2. Selected bond lengths and angles are given in Table 2. Although Kumar et al. [14] had previously isolated a Cu(II) complex of hncH, their assignment of the structure isolated is quite different to that reported herein. The metal center in **1** exhibits octahedral geometry, comprising two bidentate hnc^- ligands and two monodentate water ligands. The water molecules are *trans* to one another with Cu–O (water) bond lengths of 1.9557(14) and 1.9957(13) Å to O11 and O12, respectively, and an O12–Cu–O11 bond angle of 177.76(6)°. The hnc^- ligands are coordinated to the metal via the deprotonated hydroxy group and one oxygen of the nitro group. The geometry of the ligands relative to one another is *trans*, as is the geometry of the individual binding sites relative to one another [O5–Cu–O10 179.37(5), O1–Cu–O6 176.96(5)°]. The Cu–O (hnc) bond lengths are unremarkable as they lie in a similar range to previously reported distances [32,33]. The packing structure diagram for **1** (Fig. 3), illustrates the extent of hydrogen-bonding in the gross array, with the lactone

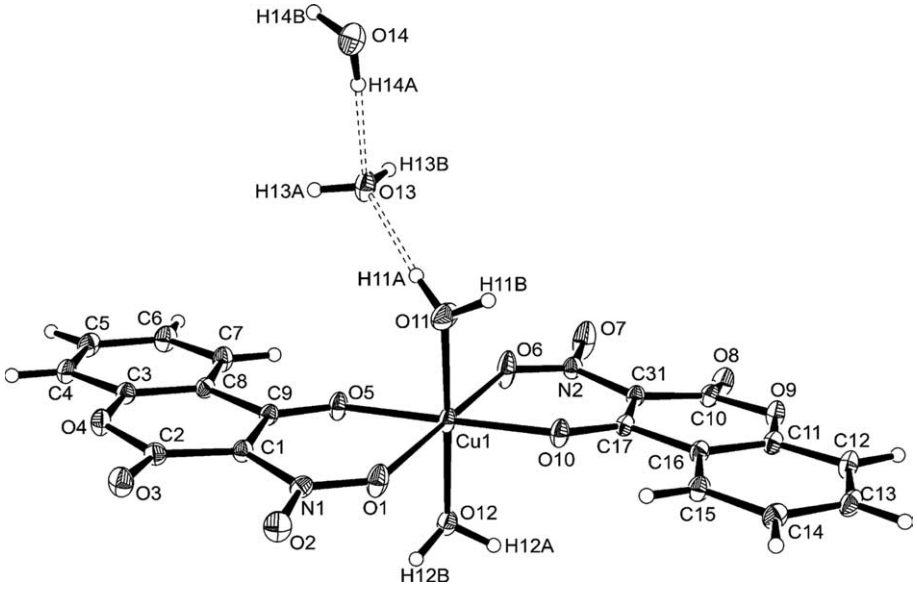

Fig. 2. Crystal structure of $[Cu(hnc)_2(H_2O)_2] \cdot 2H_2O$. Ellipsoids are represented at the 30% probability level.

Table 1
Crystal data and structure refinement for **1** and **2**

Compound	**1**	**2**
Empirical formula	$C_{18}H_{16}CuN_2O_{14}$	$C_9H_4AgNO_5$
Formula weight	547.87	314.00
Crystal system	monoclinic	monoclinic
Space group	P_1/c	P_1/c
Unit cell dimensions		
a (Å)	8.7610(1)	8.8770(1)
b (Å)	15.1230(2)	6.7120(1)
c (Å)	15.8230(2)	14.4640(2)
β (°)	103.489(1)	101.899(1)
U (Å^3)	2038.60(4)	843.28(2)
Z	4	4
D_c (g cm^{-3})	1.785	2.473
μ (mm^{-1})	1.156	2.394
F (000)	1116	608
Crystal size (mm)	$0.30 \times 0.13 \times 0.13$	$0.35 \times 0.30 \times 0.10$
θ Range for data collection (°)	3.78–30.01	4.18–30.03
Index ranges	$-12 \leqslant h \leqslant 12$; $-21 \leqslant k \leqslant 21$; $-22 \leqslant l \leqslant 22$	$-12 \leqslant h \leqslant 12$; $-9 \leqslant k \leqslant 9$; $-20 \leqslant l \leqslant 20$
Reflections collected	39853	17349
Independent reflections [R_{int}]	5916 [0.0388]	2460 [0.0477]
Reflections observed ($I > 2\sigma(I)$)	5168	2351
Absorption correction	semi-empirical from equivalents	semi-empirical from equivalents
Maximum and minimum transmission	0.90, 0.83	0.79, 0.65
Data/restraints/parameters	5916/8/349	2460/0/146
Goodness-of-fit on F^2	1.054	1.127
R_1, wR_2 [$I > 2\sigma(I)$]	0.0329, 0.0853	0.0271, 0.0708
R indices (all data)	0.0409, 0.0894	0.0299, 0.0719
Largest difference in peak and hole (e Å^{-3})	0.661, −0.560	1.071, −1.686

carbonyl and the nitro group interacting with the lattice water molecules which are, in turn, involved in hydrogen-bonding to the two ligated waters. This extensive H-bonding within the crystal could account for the observed shift in the IR carbonyl stretching frequency.

3.3. X-ray crystal structure of [Ag(4-OH-3-NO$_2$-C)] (**2**)

The X-ray crystal structure of **2** is shown in Fig. 4 and selected geometric data are given in Table 3. The complex is polymeric, with each silver having seven contacts within its coordination sphere and being bonded to four separate coumarin molecules. In particular, within the asymmetric unit there is one axial Ag–O(O1) and one equatorial Ag–O(O5) bond, at 2.5102(17) and 2.3531(16) Å, respectively. Axial metal coordination is completed by an Ag–C6 interaction (2.527(2) Å) to the coumarin moiety generated by the $1 - x$, $1/2 + y$, $1/2 - z$ symmetry operation. While this Ag–C bond is interesting, comparable interactions have been

Table 2
Selected bond lengths (Å) and angles (°) for $[Cu(hnc)_2(H_2O)_2] \cdot 2H_2O$ (**1**)

Cu(1)–O(10)	1.9300(11)	Cu(1)–O(5)	1.9304(11)
Cu(1)–O(11)	1.9557(14)	Cu(1)–O(12)	1.9957(13)
Cu(1)–O(6)	2.2764(13)	Cu(1)–O(1)	2.3254(12)
O(10)–Cu(1)–O(5)	179.37(5)	O(10)–Cu(1)–O(11)	89.42(5)
O(5)–Cu(1)–O(11)	90.23(6)	O(10)–Cu(1)–O(12)	91.51(5)
O(5)–Cu(1)–O(12)	88.86(5)	O(11)–Cu(1)–O(12)	177.76(6)
O(10)–Cu(1)–O(6)	79.51(5)	O(5)–Cu(1)–O(6)	100.00(5)
O(11)–Cu(1)–O(6)	94.54(7)	O(12)–Cu(1)–O(6)	87.63(6)
O(10)–Cu(1)–O(1)	102.40(4)	O(5)–Cu(1)–O(1)	78.11(5)
O(11)–Cu(1)–O(1)	87.86(6)	O(12)–Cu(1)–O(1)	89.95(5)
O(6)–Cu(1)–O(1)	176.96(5)		

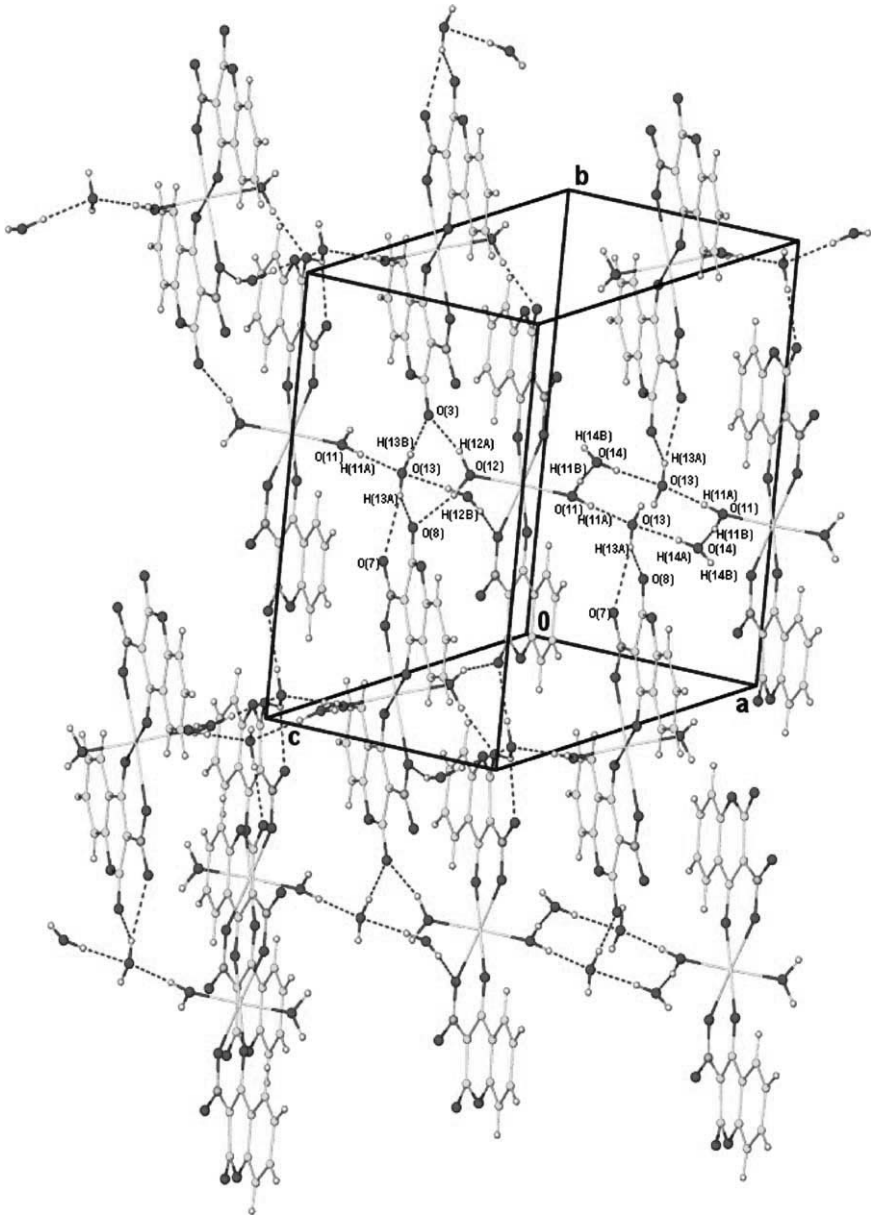

Fig. 3. Crystal packing structure of $[Cu(4\text{-hnc})_2(H_2O)_2] \cdot 2H_2O$.

previously reported for Ag(I) polycyclic aromatic complexes [39]. In the equatorial plane, each silver is also coordinated to two lactone oxygens (O3) from neighbouring molecules in the lattice. [Ag–O3[a] 2.4733(15), Ag–O3[b] 2.4970(16) Å; [a]symmetry operator $-x$, $1/2 + y$, $1/2 - z$, [b]symmetry operator x, $-1/2 - y$, $z - 1/2$]. There are also two potential longer contacts to the metal in the equatorial plane. [Ag–O2[b] 2.6784(17), Ag–O4[c], 2.7841(13) Å; [b]symmetry operator $-x$, $1/2 + y$, $z - 1/2$, [c]symmetry operator x, $-1/2 - y$, $1/2 - z$]. Bond distances for Ag–O_{OH}, Ag–$O_{C=O}$, Ag–O_{NO} and Ag–C are similar to others previously reported [34–36]. The axial bond angles of the C6‴(aryl)–Ag–O1 (nitro) (172.5°), the O5(hydroxy)-Ag–O3′(carbonyl) (72°) and O5(hydroxy)–Ag–O1(nitro) (66.8°), as well as others given in Table 3, suggests that the geometry at the metal centre is best described as a distorted pentagonal bipyramid.

3.4. Antimicrobial results

The metal-free ligands and complexes were screened for their in vitro antimicrobial activities against selected Gram positive bacteria {*S. aureus* (SA), *methicillin-resistant S. aureus* (MRSA), *S. simeoleus* (S.Sim.), *M. luteus* (Ml)} and Gram negative bacteria {*E. coli* (E.Coli), *B. olenius* (BO), *P. agglumerans* (PA)} and also against the pathogenic fungus *C. albicans* (Can). The results are presented in Table 4 as MIC_{80} values (in μM) which is the minimum concentration required to inhibit 80% of the growth of the microbe at 30 °C.

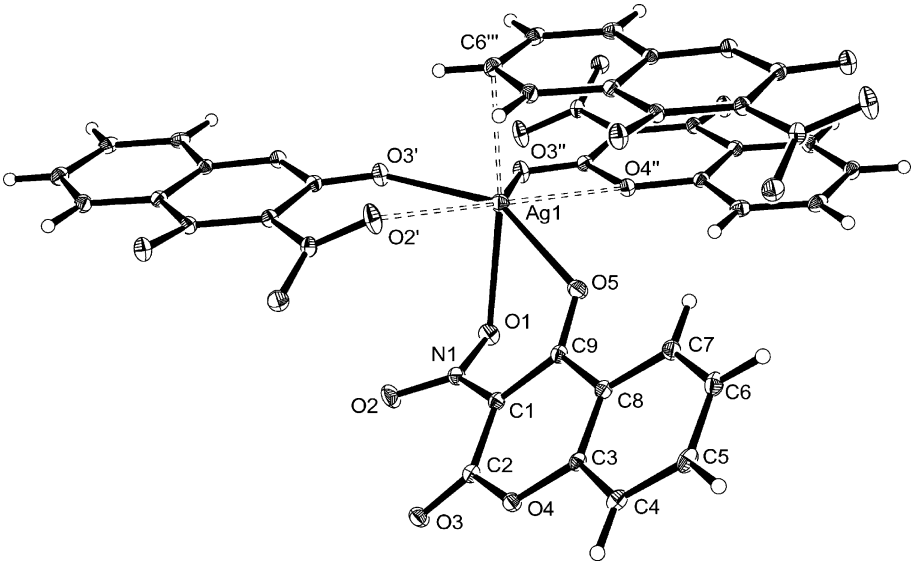

Fig. 4. Crystal structure of [Ag(4hnc)]. Ellipsoids are represented at the 30% probability level. Atoms in asymmetric unit denoted by unprimed labels. Singly, doubly and triply primed atom labels denote atoms generated via the $1 - x$, $1/2 + y$, $1/2 - z$, $-x$, $1/2 + y$, $1/2 - z$ and x, $-1/2 - y$, $-1/2 + z$ symmetry operations.

Table 3
Selected bond lengths (Å) and angles (°) for [Ag(hnc)] (**2**)

Ag(1)–O(5)	2.3531(16)	Ag(1)–O(3)#1	2.4733(15)
Ag(1)–O(3)#2	2.4970(16)	Ag(1)–O(1)	2.5102(17)
Ag(1)–C(6)#3	2.527(2)	C(6)–Ag(1)#6	2.527(2)
O(3)–Ag(1)#4	2.4733(15)	O(3)–Ag(1)#5	2.4970(16)
O(5)–Ag(1)–O(3)#1	148.98(5)	O(5)–Ag(1)–O(3)#2	123.85(6)
O(3)#1–Ag(1)–O(3)#2	71.79(6)	O(5)–Ag(1)–O(1)	66.80(5)
O(3)#1–Ag(1)–O(1)	89.93(5)	O(3)#2–Ag(1)–O(1)	86.43(5)
O(5)–Ag(1)–C(6)#3	117.14(6)	O(3)#1–Ag(1)–C(6)#3	83.99(6)
O(3)#2–Ag(1)–C(6)#3	95.79(7)	O(1)–Ag(1)–C(6)#3	172.50(6)
		Ag(1)#4–O(3)–Ag(1)#5	108.21(6)

Table 4
Antimicrobial activity given as the concentration of compound required to inhibit cell growth by 80% [MIC_{80} (μM)]

Compound	SA	MRSA	S.Sim	Ml	E.Coli	BO	PA	*C. albicans* 10231
HncH	>500	>500	>500	>500	>500	>500	>500	>500
HmnH	>500	>500	>500	>500	>500	>500	>500	>500
1,10-Phen	23.9	14.7	20	29.8	>500	>500	41.4	15
$Cu(ClO_4)_2 \cdot 6H_2O$	>500	>500	>500	>500	>500	>500	>500	>500
$AgNO_3$	69.4	124.1	16.9	64.6	69.5	31.4	67.7	66.8
1	>500	>500	>500	>500	>500	>500	>500	>500
2	143.3	114.6	124.2	70.1	41.1	82.8	117.8	219.6
3	129.3	32.6	141.1	59.4	151.6	136.9	157.4	246.6
4	32.1	2.2	16.9	16.0	44.7	16.9	15.3	4.5

The metal-free ligands, $[Cu(hnc)_2(H_2O)_2] \cdot 2H_2O$ (**1**) and the simple Cu(II) salt showed no significant antibacterial or antifungal activity. For the silver-containing samples the antimicrobial activity of the simple salt $AgNO_3$ was, almost without exception, superior to that of [Ag(hnc)] (**2**) and [Ag(hmnc)] (**3**) across all of the bacterial and the fungal species studied. However, one interesting exception to that trend was in the activity of complexes **2** and **3** against the clinically important bacterium MRSA. [Ag(hmnc)] (**3**) was approximately four times more active that $AgNO_3$ against MRSA. In general however, the phen-containing complex $[Ag(phen)_2hnc]$ (**4**) displayed the greatest inhibitory effects against all of the microbes studied, with its performances against the bacterium MRSA and the fungal isolate *C. albicans* being the most emphatic. The phen ligand itself also showed considerable activity against test strains, but complex **4** was still six times more active against MRSA and three times more active against *C. albicans*, than phen and was compara-

ble in activity to the commercially available fungicides clortrimazole and ketoconazole ($MIC_{80} = 5.5$ and 25 μM, respectively). We and others have reported the anti-*Candida* activity of several other phen complexes [37–39]. The activity of phen complexes is believed to be related to the abstraction by the phen ligands of metal ions present in trace amounts in the growth media, and that it is the resulting metal-phen complexes that are responsible for the high anti-*Candida* activity. The present work has shown that while the presence of phen in a complex does indeed increase the anti-*Candida* activity of the resulting complex, it is likely that the coumarin-metal moieties have a role to play as well.

4. Conclusions

The results presented here demonstrate that a number of potent anti-bacterial and antifungal agents have been synthesised. In particular, [$Ag(phen)_2hnc$] (**4**) shows good activity against methicillin-resistant *S. aureus* (MRSA) but not against the drug susceptible variant *S. aureus*. Complex **4** is also active against *C. albicans* and is more potent than metal-free phen. Since MRSA is frequently associated with superficial infections of wounds and ulcers the ability of **4** to inhibit the growth of MRSA might indicate a possible clinical use for the complex. It is possible that the complex compound could be incorporated into an ointment or cream for topical application to the affected area to retard the development and dissemination of infection. **4** is active against *C. albicans* and compares favourably with some of the conventional anti-fungal agents, such as clortrimazole and ketoconazole. With drug-resistant strains of microbes increasing in importance in the clinical setting, these new compounds may offer alternative candidates to those compounds presently in clinical use. A study is currently under way to elucidate the mechanism of action of the most active compounds.

5. X-ray crystallography

Single crystals of **1** and **2** were analysed at 150 K using a Nonius Kappa CCD diffractometer equipped with graphite monochromated Mo Kα radiation. Details of the data collections, solutions and refinements are given in Table 1. Both structures were solved using SHELXS-97 [29] and refined using full-matrix least-squares in SHELXL-97 [30]. Convergence was uneventful, with the following points of note.

The asymmetric unit in **1** was seen to contain two molecules of water in addition to one full molecule of the copper complex. The water hydrogen atoms were all located and refined at distances of 0.89 Å from the relevant parent atoms. In **2** the asymmetric unit is comprised of one full ligand moiety, bonded in bidentate fashion to a silver atom. Both refinements were implemented using full-matrix least-squares.

Crystallographic data for **1** and **2** have been deposited with the Cambridge Crystallographic Data Centre as supplementary publications CCDC 253929 and 253930, respectively. Copies of the data can be obtained free of charge on application to CCDC, 12 Union Road, Cambridge CB2 1EZ, UK [fax: (+44) 1223 336033, e-mail: deposit@ccdc.cam.ac.uk].

References

[1] J.W. Suttie, Clin. Cardiol. 13 (VI) (1990) 16.
[2] A.H. Bedair, N.A. El-Hady, M.S. Abd El-Latif, A.H. Fakery, A.M. El-Agrody, Il Farmaco 55 (2000) 708.
[3] T. Patonay, G. Litkei, R. Bognar, J. Eredi, C. Miszti, Pharmazie 39 (1984) 86.
[4] C. Gnerre, M. Catto, F. Leonetti, P. Weber, P.A. Carrupt, C. Altomare, A. Carotti, B.J. Testa, Med. Chem. 43 (2000) 4747.
[5] D.A. Egan, P. James, D. Cooke, R. O'Kennedy, Cancer Lett. 118 (1997) 201.
[6] M. Jiménez, J.J. Mateo, R. Mateo, J. Chrom. A 870 (2000) 473.
[7] C. Xin Zhang, S. Lippard, Curr. Opin. Chem. Biol. 7 (2003) 481.
[8] H. Sakurai, Y. Kojima, Y. Yoshikawa, K. Kawabe, H. Yasui, Coord. Chem. Rev. 226 (2002) 187.
[9] P.J. Sadler, H. Li, H. Sun, Coord. Chem. Rev. 185–186 (1999) 689.
[10] H. Ali, J.E. van Lier, Chem. Rev. 99 (1999) 2379.
[11] A.Y. Louie, T.J. Meade, Chem. Rev. 99 (1999) 2711.
[12] W.A. Volkert, T.J. Hoffman, Chem. Rev. 99 (1999) 2269.
[13] B.B. Kumar, V.J. Raju, V. Ranabaore, M.C. Ganorkar, Oriental J. Chem. 3 (1987) 34.
[14] B.B. Kumar, V.J. Raju, V. Ranabaore, J. Arch. Chem. 4 (1986) 35.
[15] I. Manolov, I. Kostova, T. Netzeva, S. Konstantinov, M. Karaivanova, Arch. Pharm. Pharm. Med. Chem. 333 (2000) 93.
[16] I. Kostova, I. Manolov, I. Nicolova, N. Danchev, Il Farmaco 56 (2001) 707.
[17] I. Pencheva, I. Kostova, S. Konstantinov, E. Naidenova, M. Karaivanova, I. Manolov, Acta Pharm. 48 (1998) 127.
[18] I. Kostova, I. Manolov, G. Momekov, Eur. J. Med. Chem. 39 (2004) 765.
[19] I. Kostova, I. Manolov, I. Nicolova, S. Konstantinov, M. Karaivanova, Eur. J. Med. Chem. 36 (2001) 339.
[20] I. Kostova, I. Manolov, M. Karaivanova, Arch. Pharm.Pharm. Med. Chem. 334 (2001) 157.
[21] M. Nath, R. Jairath, G. Eng, X. Song, A. Kumar, J. Organomet. Chem. 690 (2005) 134–144.
[22] G.J. Finn, B.S. Creaven, D.A. Egan, Melan. Res. 11 (2001) 461.
[23] G.J. Finn, E. Kenealy, B.S. Creaven, D.A. Egan, Cancer Lett. 183 (2002) 61.
[24] G. Finn, B.S. Creaven, D.A. Egan, Cancer Lett. 205 (2003) 69.
[25] G. Finn, B.S. Creaven, D.A. Egan, Cancer Lett. 214 (2004) 43.
[26] G. Finn, B.S. Creaven, D.A. Egan, Biochem. Pharm. 67 (2004) 1779.
[27] G. Finn, B.S. Creaven, D.A. Egan, Eur. J. Pharm 481 (2003) 159.
[28] D. Egan, P. James, D. Cooke, R. O'Kennedy, Cancer Lett. 118 (1997) 201.
[29] G.M. Sheldrick, SHELX-86. Program for the Solution of Crystal Structures, University of Göttingen, Germany, 1986.

[30] G.M. Sheldrick, SHELX-97. Program for Crystal Structure Refinement, University of Göttingen, Germany, 1997.
[31] I. Georgieva, T. Mihaylov, G. Bauer, N. Trefafilova, Chem. Phys. 300 (2004) 119.
[32] F. Tuna, G.I. Pascu, J.P. Sutter, M. Andruh, S. Golhen, J. Guillevic, H. Pritzkow, Inorg. Chim. Acta 342 (2003) 131.
[33] A.F. Stassen, W. Driessen, J.G. Hassnoot, J. Reedijk, Inorg. Chim. Acta 350 (2003) 57.
[34] K.M. Chi, K.H. Chen, H.C. Lin, K.J. Lin, Polyhedron 16 (1997) 2147.
[35] M. Munakata, L.P. Wu, G.L. Ning, Coord. Chem. Rev. 198 (2000) 171.
[36] M. Munakata, M. Wen, Y. Suenga, T. Kuroda-Sowa, M. Maekawa, M. Anahata, Polyhedron 20 (2001) 2321.
[37] M. McCann, M. Devereux, M. Geraghty, D. O'Shea, J. Mason, L. O'Sullivan, Metal-Based Drugs 7 (2000) 185.
[38] M. McCann, B. Coyle, S. McKay, P. McCormack, K. Kavanagh, M. Devereux, V. McKee, R. O'Gorman, M. Clynes, Biometals 16 (2003) 321.
[39] I. Druta, R. Dannac, M. Ungureanu, G. Grosu, G. Drochioiu, Ann. Pharm. Fr. 60 (2003) 321.